European Review for Medical and Pharmacological Sciences 2016; 20: 2209-2220

Identification of pathway-related modules in high-grade osteosarcoma based on topological centrality of network strategy

B. NING, D.-L. XU, J.-H. GAO, L.-L. WANG, S.-Y. YAN, S. CHENG

Department of Orthopaedics, People's Hospital of Dongying, Dongying, Shandong Province, China

Abstract. – OBJECTIVE: The objective of this paper is to identify pathway-related modules which are defined as in high-grade osteosarcoma based on topological centralities analysis of networks.

MATERIALS AND METHODS: Co-expression network was constructed by weighted gene co-expression network analysis (WGCNA) based on differentially expressed genes (DEGs). Pathway enrichment analysis was conducted by Kyoto Encyclopedia of Genes and Genomes (KEGG) database to detect pathway enriched genes. Pathway-related modules of pathway enriched genes were mined from the co-expression network. Then topological centralities (degree, closeness, stress and betweenness centrality) analyses for co-expression network and sub-networks were performed to explore hub genes. Validation of hub genes was carried out utilizing reverse transcription-polymerase chain reaction (RT-PCR) assays.

RESULTS: There were 129 nodes and 1229 edges in co-expression network. We obtained a total of 16 hub genes and 11 pathway-related modules. Module 17 (Bladder cancer module) was the most significant module, which comprising 9 of 16 hub genes and 6 pathway enriched genes, taking intersection elements (CAV1 and CCND1). RT-PCR results showed that both of CAV1 and CCND1 in high-grade osteosarcoma were significantly differentially expressed compared with normal controls.

CONCLUSIONS: This work may contribute to understanding the molecular pathogenesis and provide potential biomarkers for detections and effective therapies of high-grade osteosarcoma.

Key Words:
High-grade osteosarcoma, Topological centrality, Hub gene, Pathway, Co-expression network, Reverse transcription-polymerase chain reaction.

Introduction

High-grade osteosarcoma distinguished by the production of osteoid and immature bone is the most prevalent primary malignant bone tumor[1]. It occurs mostly in adolescents where the proliferation is most active, with a second peak in patients older than 40 years[2]. The five-year survival rate has been improved to approximately 65% in patients with no clinically detectable metastases, however, near 45% of all patients still die from osteosarcoma distant metastasis[3]. Apart from preoperative chemotherapy, no additional treatment has been investigated to increase survival significantly[4]. Equipping with better knowledge on biological markers and pathology of high-grade osteosarcoma may provide new possible targeted treatments for this tumor.

Several molecular markers, such as oncogene, tumor suppressor gene, matrix protease and growth factor families, are being identified as biological indicators in high-grade osteosarcoma[5,6]. For example, Park et al[7] suggested that *CXCR4* was involved in the higher-grade osteosarcoma and its antagonists might actually prevent distant metastasis and tumor progression. In addition, Kuijjer et al[8,9] had provided gene expression profiles of high-grade osteosarcoma with accessing number GSE33382 which were functional and useful, and showed that IGF1R signaling was active and that dual inhibition of IR/IGF1R inhibited downstream signaling and proliferation of these cells in high-grade osteosarcoma. These studies mainly focused on individual genes, probably researches based on network strategy for the expression dataset GSE33382 needed to be supplemented.

Network can provide significant instructions for mining unknown connections in incomplete networks. Although the data of large-scale protein interaction are keeping accumulated with the development of high throughput testing technology, a certain number of significant interactions are not tested, such as key genes in significant pathways[10]. This type of difficulty might be

Corresponding Author: Bo Ning, MD; e-mail: boning2015@yeah.net

resolved to some extent by utilizing sub-networks or modules of the complex network[11,12]. Hence, in the current study, we identified modules from the co-expression network of enriched genes in significant pathways and defined the modules as pathway-related modules.

The objective of this paper is to identify pathway-related modules in high-grade osteosarcoma based on topological centralities of networks and pathway enrichment analysis. To achieve this goal, we identified differentially expressed genes (DEGs) between normal controls and high-grade osteosarcoma, and performed Kyoto Encyclopedia of Genes and Genomes (KEGG) pathway enrichment analysis for DEGs. Next, co-expression network was constructed by weighted gene co-expression network analysis (WGCNA), and then pathway-related modules which included DEGs enriched in significant pathways were mined. Then topological centralities (degree, closeness, stress and betweenness centrality) were conducted for network and modules to explore hub genes. Finally, hub genes in pathway-related modules were validated by reverse transcription-polymerase chain reaction (RT-PCR) assays.

Materials and Methods

Data Recruitment

In the present paper, microarray gene expression profile deposited in the Gene Expression Omnibus (GEO) database with accessing number GSE33382 [8, 9] was recruited. GSE33382 comprised a total of 87 samples, including 84 high-grade osteosarcoma samples and 3 normal samples. The expression profile existed on Illumina human-6 v2.0 expression beadchip (using nuIDs as identifier) platform and consisted of 48701 nuIDs.

Detection of DEGs

To identify DEGs between high-grade osteosarcoma and normal controls, Linear Models for Microarray Data (Limma) package was utilized[13]. Only the genes with false discovery rate (FDR) adjusted p-values < 0.05 and |logFoldChange| > 2 were considered to be DEGs. Then nuIDs of DEGs were converted into gene symbols with a medium of transformation.

Pathway Enrichment Analysis

KEGG pathway enrichment analysis for DEGs was performed based on the Database for Annotation, Visualization and Integrated Discovery (DAVID)[14]. And pathways which met the criterion $p < 0.05$ were selected according to expression analysis systematic explorer (EASE) test implemented in DAVID[15]. The calculating formula of EASE was shown as following:

$$p = \frac{\binom{a+b}{a}\binom{c+d}{c}}{\binom{n}{a+c}}$$

Of which $a = a'$-1, a' was the gene number of one gene set in the gene lists; $a' + b$ was the number of genes in the gene list including at least one gene set; $a' + c$ was the gene number of one gene list in the background genes; $n = a' + b + c + d$ was the number of background genes in EASE.

Co-expression Network Construction

Gene co-expression network is instrumental for describing the pair-wise relationships among genes and facilitates the understanding of their function and identification of their significant players[16]. In this paper, WGCNA[17], a system biology methods which provides a comprehensive set of functions for performing a correlation network analysis of large high-dimensional data sets, was applied to describe correlation patterns among DEGs of high-grade osteosarcoma. Genes were denoted as nodes of a gene co-expression network and correlations between gene pairs are presented as edges. The first step was to define co-expression similarity S_{ij} for each pair of genes x_i and x_j. A signed co-expression measure between x_i and x_j was used to preserve the sign of the correlation which was defined with a simple transformation of the correlation:

$$S_{ij} = \frac{1 + cor(x_i, x_j)}{2}$$

In addition, the difference of signed and unsigned similarities lies in how they treated negatively correlated genes. There will be a high similarity in an unsigned network of genes with a high negative correlation while a low similarity in a signed network.

Then, the co-expression similarity matrix $S = [S_{ij}]$ was transformed into the adjacency matrix $A = [a_{ij}]$, which fully specified the network and en-

coded the network connection strength between nodes, using a thresholding procedure. For an un-weighted network, the adjacency was defined to be 1 (a_{ij} = 1) and 0 otherwise if the absolute correlation between their expression profiles was above a pre-defined threshold τ and were deemed separated otherwise, as following:

$$a_{ij} = \begin{cases} 1 & if\ S_{ij} \geq \tau \\ 0 & otherwise \end{cases}$$

The hard thresholding of un-weighted networks may loss the continuous nature of the underlying co-expression information[17]. In contrast, a soft thresholding of weighted network adjacency defined by raising the co-expression similarity S_{ij} to a power β ≥ 1 was needed. It could allow the adjacency to take on values in succession between 0 and 1 to preserve continuous nature of the co-expression information. The continuous measure to assess gene connection strength was given as:, and the weighted adjacency a_{ij} between two genes was proportional to their similarity in the following formula.

$$\log(a_{ij}) = \beta \times \log(S_{ij})$$

Pathway-related Modules Mining

In this study, pathway-related modules were extracted from co-expression network to explore significant genes and modules which played key roles in the progression of high-grade osteosarcoma. To achieve this, we firstly explored the same genes between significant pathways and co-expression network; then extracted these genes related sub-networks with thresholds of nodes cutoff = 10; finally, conducted topological analysis to evaluate significant pathway-related modules.

Topological Analysis

One of the fundamental problems in network analysis is to determine the importance of a particular vertex or an edge in a network[18]. Quantifying centrality and connectivity help identify portions of the network that may play interesting roles. Researchers have revealed that topological centrality is shown to be effective for identifying essential molecules in well-characterized interaction networks[19]. We presented centrality of the co-expression network on the local scale (degree), and the global scale (closeness, stress and betweenness). The genes at the ≥ 95% quantile distribution in the significantly perturbed networks were defined as hub genes.

To evaluate centrality of a co-expression network, we should define several preliminaries. For a graph $G = (V, E)$, where V was the set of vertices representing nodes in the network, and E was the set of edges representing the relationships between the actors. A path from node s to t was defined as a sequence of edges and the length of a path was the sum of the weights of edges. We used $d(s, t)$ to denote the distance between s and t (the minimum length of any path connecting s and t in G). Let us denote the total number of shortest paths between vertices s and t by σ_{st}, and the number passing through node v by $\sigma_{st}(v)$.

Degree Centrality

Degree centrality is a simple local measure, based on the notion of neighborhood. This index is useful in case of static graphs, for situations when we are interested in finding vertices that have the most direct connections to other vertices. Degree centrality quantifies the local topology of each gene by summing up the number of its adjacent genes[20].

Closeness Centrality

Closeness centrality, $C_c(v)$, is a measure of the average length of the shortest paths to access all other proteins in the network[21]. It was defined as the reciprocal of the average shortest path length:

$$C_C(v) = \frac{1}{\sum_{t \in N} d(s,t)}$$

Stress Centrality

This index computes the number of nodes in the shortest path between two other nodes[22]. If a node was stressed, it would be traversed by a high number of shortest paths. The stress, $C_s(v)$ was defined as:

$$C_S(v) = \sum_{s \neq v \in N} \sum_{t \neq v \in N} \sigma_{st}(v)$$

Betweenness Centrality

Betweenness centrality, $C_B(v)$, is a shortest paths enumeration-based metric in graphs for determining how the neighbors of a node are inter-

Table I. Sequences of primers and length for 5 candidate genes.

Gene	Primers (5′-3′) Forward	Reverse	Length bp
CAV1	CTGTCGGAGCGGGACATCT	GCCTTCCAAATGCCGTCAAA	241
IGFBP2	ATCCCCAACTGTGACAAGCA	ATGCAAAAGGGACACAGGGG	515
FCGR2A	TTTGTTGCTCCTCTCCTTCTG	ATCTTGCTCGCCATAGTGGT	392
CXCL1	AGCTCTTCCGCTCCTCTCAC	GGACGCTCCTAGGGAAGAAGA	178
CCND1	CCTCTTCACCTTATTCATGGCTGA	CGTATCGTAGGAGTGGGACAGGT	192
β-actin	AAGTACTCCGTGTGGATCGG	TCAAGTTGGGGGACAAAAAG	615

connected, and is considered the ratio of the node in the shortest path between two other nodes [23], in consequence $C_B(v)$ ε [0, 1]. It was calculated as following:

$$C_B(v) = \sum_{s \neq v \neq t \in N} \frac{\sigma_{st}(v)}{\sigma_{st}}$$

Validation of Hub Genes

RT-PCR assays were carried out to validate hub genes of the network and sub-networks. Total RNA was prepared from 10 high-grade osteosarcoma patients using TRIzol regent (Invitrogen, Carlsbad, CA, USA). For the cDNA synthesize, RNA was treated with oligo $(dT)_{18}$ primers (Invitrogen, Carlsbad, CA, USA), 2 μL RNasin (40 U/μL), 8.0 μL 5 × reverse transcriptase buffer, 8.0 μL dNTPs and 2 μL AMV reverse transcriptase (5 U/μL). The reactions were incubated for 1 h at 42 °C, 15 min at 70°C, and adjusted to a final volume of 50 μL. The data were normalized to β-actin reference. *CAV1*, *IGFBP2*, *FCGR2A*, *CXCL1* and *CCND1* were taken as examples to conduct RT-PCR validated assays and their primer sequences were listed in Table 1.

For PCR amplification, each 4 μL reaction contained 10 μL of 10 × PCR Buffer I (Invitrogen, Carlsbad, CA, USA), 1 μL of Taq DNA Polymerase (Invitrogen, Carlsbad, CA, USA), 3 μL of each forward and reverse primer, 8 μL of dNTPs. Conditions were as follows: 1 min at 95 °C for pre-denaturation, followed by 35 cycles of 30 s at 94 °C, 30 s at 55 °C and 30 s at 72 °C, and a final 7 min extension at 72 °C. Three replicates of the assay within or between runs were performed to assess the reproducibility. Products of PCR experiment were analyzed by 1.5% agarose gel electrophoresis and Quantity One Software of gel imaging analyzer (Bio-Rad, Hercules, CA, USA).

Results

Detection of DEGs

We identified a total of 228 DEGs between high-grade osteosarcoma and normal controls with thresholds of $p < 0.05$ and |logFoldChange| > 2. Among 228 DEGs, 115 were up-regulated and 113 were down-regulated.

Pathway Enrichment Analysis

Results of KEGG pathway enrichment analysis showed 228 DEGs enriched in 19 significant pathways under the condition of $p < 0.05$ (Table 2). The most significant three pathways were type I diabetes mellitus (p = 2.08E-05), asthma (p = 2.29E-05) and intestinal immune network for IgA production (p = 5.86E-05), and they might have not obvious relationships with high-grade osteosarcoma. However, when ranking the 19 pathways in sequence of their counts, we found that pathways in cancer with 13 counts, cell adhesion molecules with 11 counts and systemic lupus erythematosus with 10 counts were top three pathways. The count value equaled to the number of DEGs enriched in one pathway, so high counts mean that the pathway included more DEGs which might play key roles in high-grade osteosarcoma.

Co-expression Network Construction and Topological Analysis

In the work, co-expression network was constructed utilizing WGCNA based on 228 DEGs of high-grade osteosarcoma. There were 129 nodes represented genes and 1299 edges which was the interaction between a pair of co-expressed genes in the co-expression network (Figure 1). Interestingly, up-regulated and down-regulated DEGs trended to co-express in small networks respectively, rather than hybrid crossover to form a global network.

To further determine the importance of nodes, topological centrality of degree, closeness, stress

Table II. Significant KEGG pathways of high-grade osteosarcoma with $p < 0.05$.

Term	Count	*p*-value	Genes
Pathways in cancer	13	3.91 E-02	*WNT5A, FGFR3, WNT5B, EPAS1, MMP9, TGFB3, ITGA2, FOXO1, BCL2L1, RALGDS, CCND1, CDKN1A, CSF1R*
Cell adhesion molecules (CAMs)	11	3.79E-04	*NRCAM, SDC4, CADM1, HLA-DRB4, ITGB2, HLA-DPA1, HLA-DMB, ALCAM, HLA-DMA, HLA-DQA1, HLA-DRA*
Systemic lupus erythematosus	10	1.92E-04	*C1QA, HLA-DRB4, HLA-DPA1, FCGR2A, HLA-DMB, C1QB, C1QC, HLA-DMA, HLA-DQA1, HLA-DRA*
Focal adhesion	10	2.36 E-02	*CAV2, VWF, COL1A1,CCND1, ITGA2, CAV1, THBS1, COL5A2, COL5A1, SPP1*
Viral myocarditis	9	9.80E-05	*CAV1, HLA-DRB4, HLA-DPA1, CCND1, HLA-DMB, HLA-DMA, ITGB2,HLA-DQA1, HLA-DRA*
ECM-receptor interaction	9	3.21E-04	*VWF, GP1BB, ITGA2, COL1A1, SDC4, THBS1, COL5A2, COL5A1, SPP1*
Hematopoietic cell lineage	9	3.77E-04	*GP1BB, HLA-DRB4, MME, ITGA2, CD9,ANPEP, CD14, HLA-DRA, CSF1R*
Type 1 diabetes mellitus	8	2.08E-05	*CPE, HLA-DRB4, HLA-DPA1, HLA-DMB, IGF2, HLA-DMA, HLA-DQA1, HLA-DRA*
Intestinal immune network for IgA production	8	*5.86E-05*	*CXCR4, HLA-DMA, HLA-DRB4, HLA-DPA1, HLA-DMB, TGFB3,HLA-DQA1, HLA-DRA*
Asthma	7	2.29E-05	*HLA-DRB4, FCER1G, HLA-DPA1, HLA-DMB,HLA-DMA, HLA-DQA1, HLA-DRA*
Complement and coagulation cascades	7	2.95 E-03	*C1QA, C1QB, VWF, A2M, SERPINE1, TFPI, C1QC*
Antigen processing and presentation	7	7.34 E-03	*HLA-DRB4, HLA-DPA1, HLA-DMB, HLA-DMA, CD74, HLA-DQA1, HLA-DRA*
Allograft rejection	6	8.07E-04	*HLA-DRB4, HLA-DPA1, HLA-DMB, HLA-DMA, HLA-DQA1, HLA-DRA*
Graft-versus-host disease	6	1.17E-03	*HLA-DRB4, HLA-DPA1, HLA-DMB, HLA-DMA, HLA-DQA1, HLA-DRA*
Autoimmune thyroid disease	6	3.93 E-03	*HLA-DRB4, HLA-DPA1, HLA-DMB, HLA-DMA, HLA-DQA1, HLA-DRA*
p53 signaling pathway	6	1.32 E-02	*CDKN1A, CCND1, ZMAT3, SERPINE1, THBS1, IGFBP3*
Bladder cancer	5	1.09 E-02	*CDKN1A, CCND1, FGFR3, MMP9, THBS1*
Steroid hormone biosynthesis	5	1.49 E-02	*AKR1C3, CYP1B1, HSD11B1, HSD17B7, AKR1C1*
Prion diseases	4	3.56 E-02	*C1QA, C1QB, CCL5, C1QC*

and betweenness analysis for co-expression network were performed. In addition, the genes at the ≥ 95% quantile distribution in the significantly perturbed networks were defined as hub genes. Results of top 5% ranked genes in co-expression network based on degree, stress, closeness and betweenness centrality analysis were displayed in Table 3. It was easy to find that hub genes or top 5% distribution genes in various centralities analyses of the same network were

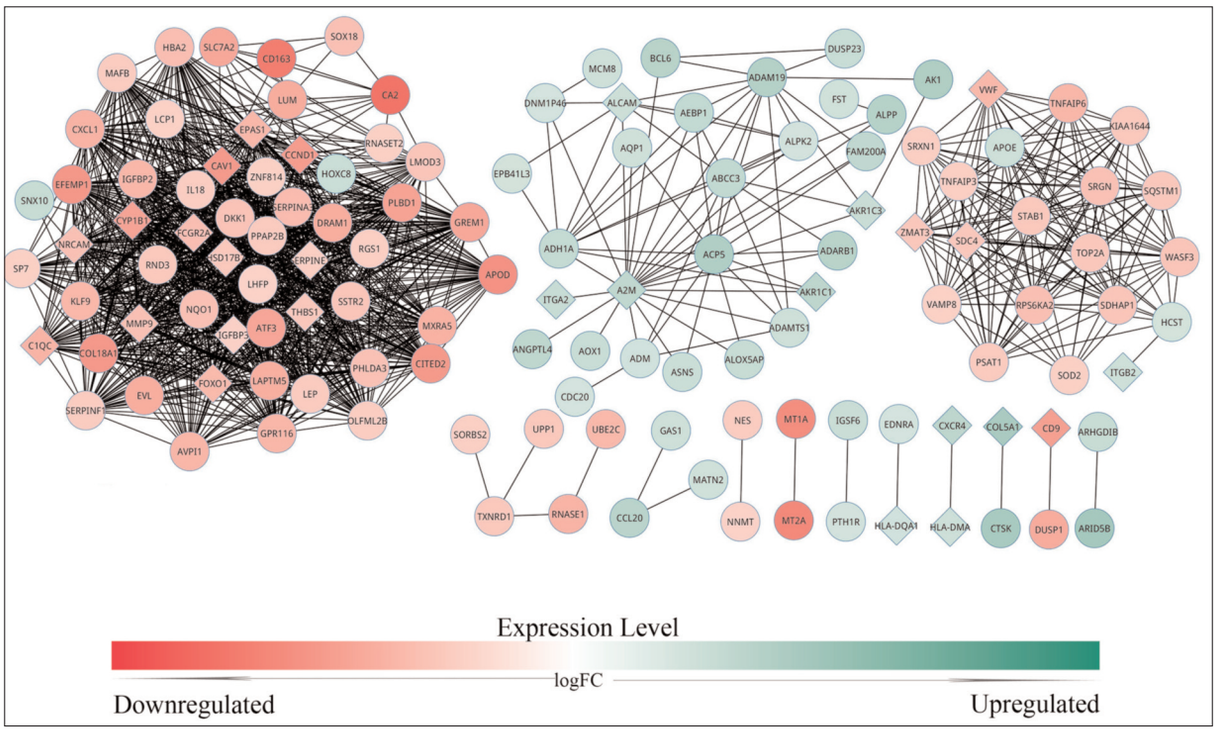

Figure 1. Co-expression network of high-grade osteosarcoma. There were 129 nodes and 1229 edges in the co-expression network which constructed by WGCNA. Nodes represented genes and edges stood for the interactions of genes. The rhombus nodes were genes enriched in significant pathways. The color of one node was decided by logFoldChange (logFC) value of the gene. The darker of a node, the bigger of |logFC| was.

not entirely consistent. We obtained total 16 hub genes by integrating results of the four types of centralities, among which 6 were pathway enriched genes (*CAV1*, *CCND1*, *FCGR2A*, *A2M*, *HLA-DMA* and *SDC4*). In detailed, hub genes which had been identified by more than one centrality analysis were regarded as common hub genes, which including *CAV1*, *CCND1*, *CXCL1*, *FCGR2A*, *A2M* and *CCL20* in this study.

Pathway-Related Modules Mining and Topological Analysis

Among 129 DEGs mapped to the network, 16 genes (*HLA-DQA1*, *HLA-DMA*, *CXCR4*, *CAV1*, *CCND1*, *ITGB2*, *C1QC*, *FCGR2A*, *SDC4*, *VWF*, *THBS1*, *ITGA2*, *COL5A1*, *CD9*, *NRCAM* and *ALCAM1*), which were denoted as rhombus in Figure 1, were also enriched in 19 significant pathways with $p < 0.05$. These genes might play key roles in the high-grade osteosarcoma progression and treatment. Therefore we mined the 16 pathway enriched genes related sub-networks or modules which met the criterion (node cutoff = 10), and obtained 11modules (Figure 2). To further investigate the biological functions of these modules, topological centralities analyses (degree, stress, closeness and betweenness) were carried out, as shown in Figure 3. Module 17 had the

Table III. Top 5% ranked genes in co-expression network based on centralities analyses.

Centrality	Degree		Stress		Closeness		Betweenness	
No.	Terms	Value	Terms	Value	Terms	Value	Terms	Value
1	*CAV1*	*53*	*CAV1*	*1138*	*CAV1*	*0.965*	*CCL20*	*0.911*
2	*IGFBP2*	*50*	*CXCL1*	*936*	*CCL20*	*0.960*	*TXNRD1*	*0.833*
3	*FCGR2A*	*50*	*CCND1*	*936*	*HLA-DMA*	*0.954*	*A2M*	*0.533*
4	*CXCL1*	*50*	*EPAS1*	*760*	*SDC4*	*0.950*	*RNASE1*	*0.500*
5	*CCND1*	*50*	*LUM*	*694*	*CCND1*	*0.917*	*ADAM19*	*0.138*
6	*SSTR2*	*49*	*A2M*	*668*	*FCGR2A*	*0.802*	*HCST*	*0.105*

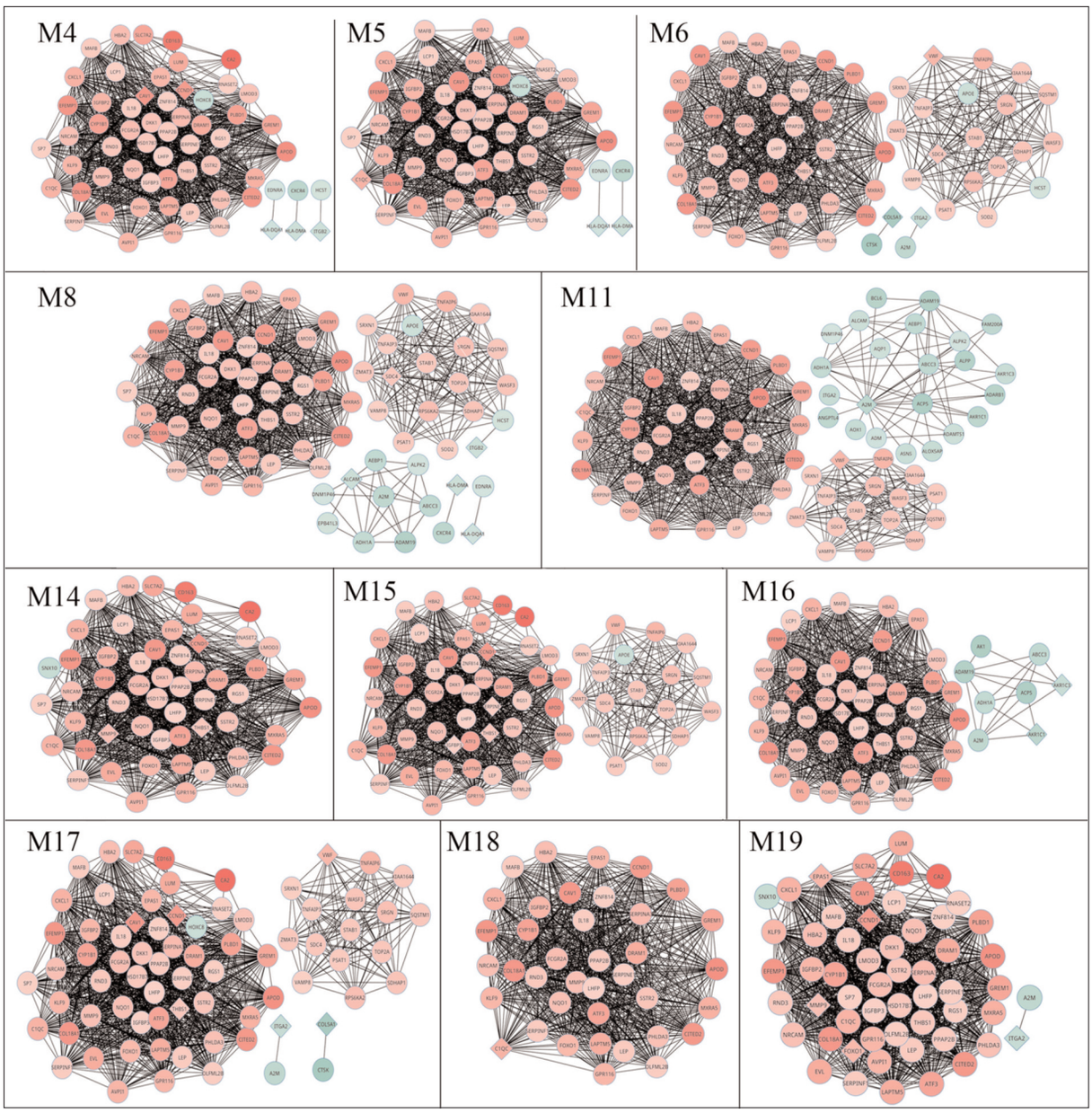

Figure 2. Pathway-related modules for genes mapped to the global network which were also enriched in significant pathways. M represented modules or sub-networks, and the subsequent number was the ID of this modules. Nodes represented genes and edges stood for the interactions of genes. The rhombus nodes were genes enriched in significant pathways. The color of one node was decided by logFoldChange (logFC) value of the gene. The darker of a node, the bigger of |logFC| was.

highest degree of 2350, closeness of 63.96 and stress of 9580, while Module 11 possessed the highest betweenness with 0.82. The Module 17 was module of bladder cancer, and Module 11 was module of complement and coagulation cascades.

Validation of hub Genes Based on RT-PCR

A total of five genes (*CAV1*, *IGFBP2*, *FCGR2A*, *CXCL1* and *CCND1*) in most significant modules were taken as examples to validate topological centrality analysis of co-expression network and examine the changes in expression levels by RT-PCR in high-grade osteosarcoma patients (Figure 4). Detailed, the five DEGs were all down-regulated genes, and *IGFBP2* was not pathway enriched gene. The results showed that, compared with normal controls, relative expression levels of all candidate genes were decreased, which confirmed to regulations of DEGs. *CAV1*,

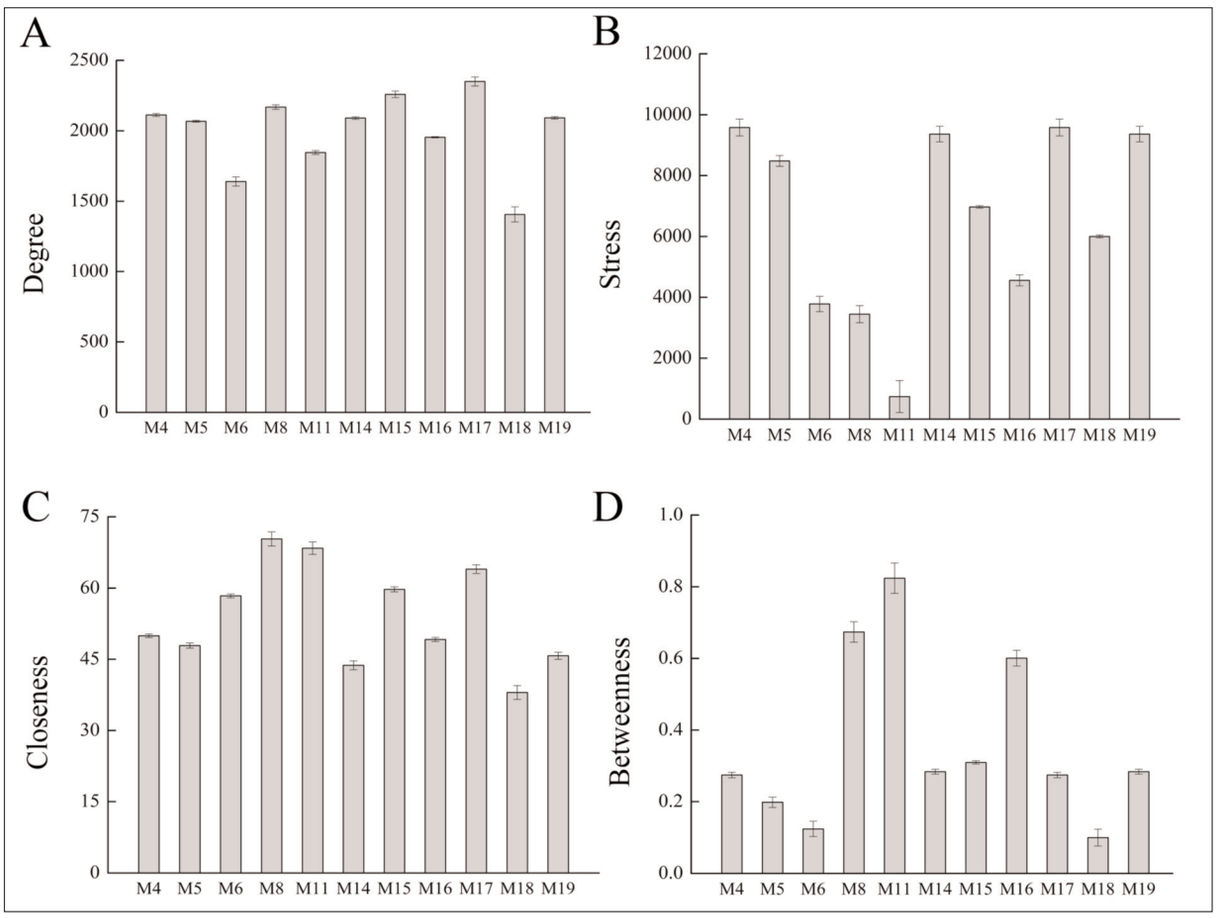

Figure 3. Topological centrality (degree, stress, closeness and betweenness) results for 11 modules. M represented modules or sub-networks, and the subsequent number was the ID of this modules.

IGFBP2 and *CCND1* in high-grade osteosarcoma patients were significantly differently expressed with $p < 0.001$, but *FCGR2A* was not differently expressed with $p > 0.05$.

Discussion

In this paper, we identified hub genes based on topological centralities (degree, closeness, stress and betweenness centrality) of co-expression network and sub-network, integrated result of the five centralities to solve the inconsistent outcomes caused by different methods, and validated hub genes by RT-PCR. For the co-expression network which constructed on the basis of 228 DEGs, there were 129 nodes and 1299 edges. We discovered an interesting phenomenon, up-regulated and down-regulated DEGs trended to co-express in small networks respectively, which might indicate the sub-networks played important roles in the progression of high-grade osteosarcoma. Furthermore, alteration of one or more pathways could affect the normal differentiation and might cause tumors[24]. Therefore, we mined pathway-related modules, including nodes enriched in significant pathways.

By accessing centralities analyses (degree, stress, closeness and betweenness centrality) for co-expression network and sub-network, we obtained a total of 16 hub genes and 11 modules. In detailed, bladder cancer module was the most significant module, which comprising 9 of 16 hub genes and 6 pathway enriched genes, taking intersection elements (*CAV1* and *CCND1*). Besides, we had validated *CAV1* and *CCND1* by RT-PCR and the results showed that both of the two genes in high-grade osteosarcoma were significantly differently expressed compared with normal controls.

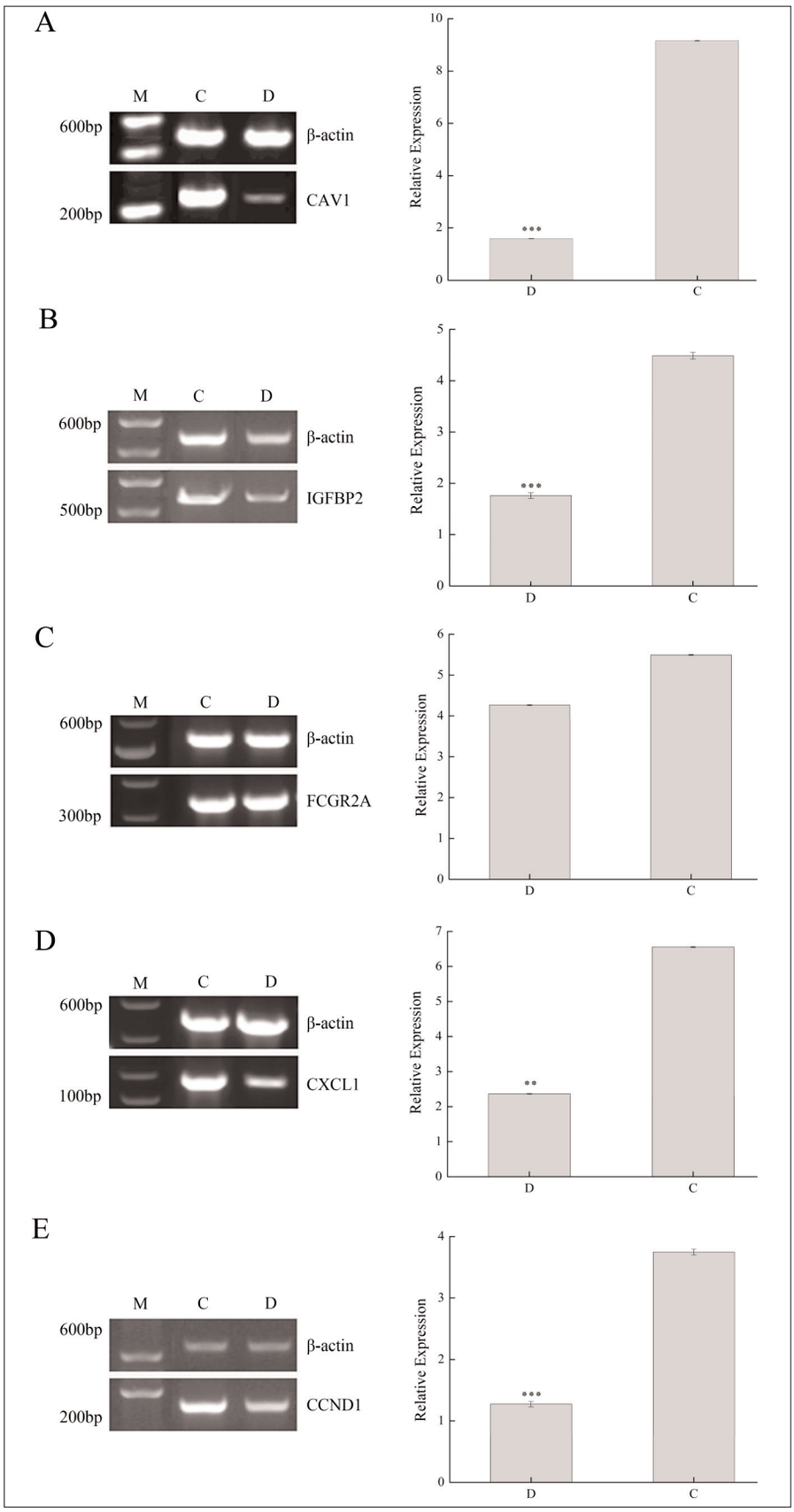

Figure 4. RT-PCR results and relative expressions for CAV1 ***(A)***, IGFBP2 ***(B)***, FCGR2A ***(C)***, CXCL1 ***(D)***, and CCND1 ***(E)***. M stood for markers, D was high-grade osteosarcoma group and C represented normal control group. The expression of one gene in high-grade osteosarcoma compared to normal controls was indicated by its p value. If one gene with p was more than 0.05, the gene would be not significantly differently expressed, in contrast, a gene of $p < 0.05$ was considered to be significantly differently expressed, $^{*}p < 0.05$, $^{**}0.05 < p < 0.001$, $^{***}p < 0.001$. Apart from FCGR2A, the other candidate genes were significantly differently expressed.

CAV1 (caveolin 1), a member of caveolin families which are membrane-bound scaffolding proteins that compartmentalize and negatively regulate signal transduction, is the major component of endocytic caveolae plasma membrane invaginations and assists in focal adhesion stabilization required for directional cell migration[25]. Recent studies [26-28] had implicated that loss of *CAV1* expression in cancer-associated fibroblasts resulted in an activated tumor microenvironment, thereby driving early tumor recurrence, metastasis, and poor clinical outcome in cancers. For example, carcinoma-associated stroma was enriched in *CAV1*, which promoted local tumor invasion and metastasis according to biomechanical remodeling analysis[27]. Moreover, *CAV1* was likely to act as a tumor suppressor gene in human sarcomas[29]. Lara et al[30] reported that *CAV1* down-regulation was part of osteoblast transformation and osteosarcoma progression and validated its role as onco-suppressor in human osteosarcoma. In the work, *CAV1* was down-regulated DEG and significantly differently expressed which were consistent with these previous studies. Therefore *CAV1* related to high-grade osteosarcoma closely.

CCND1, which encodes the cell-cycle protein cyclin D1, a member of the highly conserved cyclin family whose members are characterized by a dramatic periodicity in protein abundance through the cell cycle, is an important regulator of cell cycle progression and its over-expression has been linked to the development and progression of cancer[31], and non-coding microRNAs (miRNAs) act as crucial modulators of *CCND1*[32]. The importance of *CCND1* in osteosarcoma had previously been reported; for instance, Xu et al[33] revealed that it inhibited proliferation of bone tumor cells and played a tumor-suppressing role. It had been demonstrated that the *CCND1* contributed to osteosarcoma cell proliferation, suggesting that repression of *CCND1* might be used for osteosarcoma therapy[34]. In addition, *CCND1* transcription which was suppressed by miRNAs, directly reduced cell proliferation in osteosarcoma[35], which confirmed to our result *CCND1* enriched in p53 signaling pathway. Above all, we may infer that *CCND1* was a target for the diagnosis and treatment of high-grade osteosarcoma.

Meanwhile, we found that *CAV1* and *CCND1* were enriched in 2 pathways (focal adhesion and viral myocarditis) simultaneously. For focal adhesion, enriched genes were all consist in bladder cancer module, which indicated that this pathway might play key role in high-grade osteosarcoma. Focal adhesions, are large macromolecular assemblies through which mechanical force and regulatory signals are transmitted between the extracellular matrix and an interacting cell[36]. Focal adhesion kinase (*FAK*), a non-receptor tyrosine kinase that resides at the sites of at focal adhesions[37], has been shown to be an important mediator of cell adhesion, growth, proliferation, survival, angiogenesis and migration, all of which are often disrupted in cancer cells[38]. Over-expression of *FAK* in tumors was important for motility, angiogenesis and metastasis[39]. Schröder et al[40] suggested that altered *FAK* was observed for different tumors and could also be important for osteosarcoma development. Wang et al[41] uncovered that inhibition of *FAK* induced apoptosis in osteosarcoma cells[38], while it also involved in the migration of osteosarcoma cells. Therefore, focal adhesion was a significant biological process for osteosarcoma. Bladder cancer module was the most significant module of high-grade osteosarcoma, which revealed that there was a close correlation between two diseases. We discovered that some significant genes of them were the same, such as *CAV1* and *CCND1*[42,43]. Besides, their significant pathways also had intersections, for instance focal adhesion and ECM-receptor interaction[44]. Thus, the relationship between high-grade osteosarcoma and bladder cancer was confirmed by previous researches in certain extent.

Conclusions

We successfully identified pathway-related modules (for example, bladder cancer module) and hub genes (such as *CAV1* and *CCND1*) in high-grade osteosarcoma based on topological centralities of co-expression network, pathway enrichment analysis and validated hub genes by RT-PCR. These genes and modules might be potential biomarkers for diagnose and treatment of high-grade osteosarcoma.

Conflict of Interest

The Authors declare that they have no conflict of interests.

References

1) Campanacci M. High grade osteosarcomas. Bone and soft tissue tumors. Springer Vienna, 1999; pp. 463-515.

2) Anninga JK. Clinical and molecular features of high-grade osteosarcoma. Department of Paediatrics, Pathology, Bone Tumors, Faculty of Medicine, Leiden University Medical Center (LUMC), Leiden University, 2013.
3) Mohseny AB, Cai Y, Kuijjer M, Xiao W, van den Akker B, de Andrea CE, Jacobs R, ten Dijke P, Hogendoorn PC, Cleton-Jansen AM. The activities of Smad and Gli mediated signalling pathways in high-grade conventional osteosarcoma. Eur J Cancer 2012; 48: 3429-3438.
4) Buddingh EP, Kuijjer ML, Duim RA, Bürger H, Agelopoulos K, Myklebost O, Serra M, Mertens F, Hogendoorn PC, Lankester AC. Tumor-infiltrating macrophages are associated with metastasis suppression in high-grade osteosarcoma: a rationale for treatment with macrophage activating agents. Clin Cancer Res 2011; 17: 2110-2119.
5) Hoang BH, Kubo T, Healey JH, Sowers R, Mazza B, Yang R, Huvos AG, Meyers PA, Gorlick R. Expression of LDL receptor-related protein 5 (LRP5) as a novel marker for disease progression in high-grade osteosarcoma. Int J Cancer 2004; 109: 106-111.
6) Li H, Meng Q, Liu W, Li Y, Zhang H, Bao F, Song L, Li H. IMPDH2 mediate radioresistance and chemoresistance in osteosarcoma cells. Eur Rev Med Pharmacol Sci 2014; 18: 3038-3044.
7) Park HR, Seo J, Bacchini P, Bertoni F, Park YK. Differential expression of CXCR4 in conventional high-grade and low-grade central osteosarcoma and its prognostic implications. J Korean Bone Joint Tumor Soc 2012; 18: 20-27.
8) Kuijjer ML, Rydbeck H, Kresse SH, Buddingh EP, Lid AB, Roelofs H, Bürger H, Myklebost O, Hogendoorn PC, Meza Zepeda LA. Identification of osteosarcoma driver genes by integrative analysis of copy number and gene expression data. Gene Chromosome Canc 2012; 51: 696-706.
9) Kuijjer ML, Peterse EF, van den Akker BE, Briaire-de Bruijn IH, Serra M, Meza-Zepeda LA, Myklebost O, Hassan AB, Hogendoorn PC, Cleton-Jansen AM. IR/IGF1R signaling as potential target for treatment of high-grade osteosarcoma. BMC Cancer 2013; 13: 245-253.
10) Nibbe RK, Chowdhury SA, Koyutürk M, Ewing R, Chance MR. Protein–protein interaction networks and subnetworks in the biology of disease. Wires Syst Biol Med 2011; 3: 357-367.
11) Wu Y, Jing R, Jiang L, Jiang Y, Kuang Q, Ye L, Yang L, Li Y, Li M. Combination use of protein–protein interaction network topological features improves the predictive scores of deleterious non-synonymous single-nucleotide polymorphisms. Amino Acids 2014; 46: 2025-2035.
12) Wan F, Cui Y, Wu J, Wang J, Liu Q, Gao Z. The PPI network and cluster ONE analysis to explain the mechanism of bladder cancer. Eur Rev Med Pharmacol Sci 2013; 17: 618-623.
13) Smyth GK. Linear models and empirical bayes methods for assessing differential expression in microarray experiments. Stat Appl Genet Mol Biol 2004; 3: 1-28.
14) Huang DW, Sherman BT, Lempicki RA. Systematic and integrative analysis of large gene lists using DAVID bioinformatics resources. Nat Protoc 2008; 4: 44-57.
15) Wang X, Simon R. Microarray-based cancer prediction using single genes. BMC Bioinformatics 2011; 12: 391-400.
16) Cokus S, Rose S, Haynor D, Gronbech-Jensen N, Pellegrini M. Modelling the network of cell cycle transcription factors in the yeast Saccharomyces cerevisiae. BMC Bioinformatics 2006; 7: 381-392.
17) Zhang B, Horvath S. A general framework for weighted gene co-expression network analysis. Stat Appl Genet Mol Biol 2005; 4: 1544-6115.
18) Bader DA, Madduri K. Parallel algorithms for evaluating centrality indices in real-world networks. Parallel Processing, 2006. ICPP 2006. International Conference on 2006; 539-550.
19) Prifti E, Zucker J-D, Clément K, Henegar C. Interactional and functional centrality in transcriptional co-expression networks. Bioinformatics 2010; 26: 3083-3089.
20) Haythornthwaite C. Social network analysis: an approach and technique for the study of information exchange. Libr Inform Sci Res 1996; 18: 323-342.
21) Wasserman S. Social network analysis: Methods and applications. Cambridge University Press, 1994; p. 8.
22) Fekete SP, Kaufmann M, Kröller A, Lehmann K. A new approach for boundary recognition in geometric sensor networks. In Proceeding of the 17th Canadian Conference on Computational Geometry, 2005; pp. 82-85.
23) Barthelemy M. Betweenness centrality in large complex networks. Eur Phys J B CMCS 2004; 38: 163-168.
24) Mohseny AB, Hogendoorn PC. Concise review: mesenchymal tumors: when stem cells go mad. Stem Cells 2011; 29: 397-403.
25) Goetz JG, Joshi B, Lajoie P, Strugnell SS, Scudamore T, Kojic LD, Nabi IR. Concerted regulation of focal adhesion dynamics by galectin-3 and tyrosine-phosphorylated caveolin-1. J Cell Biol 2008; 180: 1261-1275.
26) Sotgia F, Martinez-Outschoorn UE, Howell A, Pestell RG, Pavlides S, Lisanti MP. Caveolin-1 and cancer metabolism in the tumor microenvironment: markers, models, and mechanisms. Annu Rev Pathol 2012; 7: 423-467.
27) Goetz JG, Minguet S, Navarro-Lérida I, Lazcano JJ, Samaniego R, Calvo E, Tello M, Osteso-Ibáñez T, Pellinen T, Echarri A. Biomechanical remodeling of the microenvironment by stromal caveolin-1 favors tumor invasion and metastasis. Cell 2011; 146: 148-163.
28) Goetz JG, Lajoie P, Wiseman SM, Nabi IR. Caveolin-1 in tumor progression: the good, the bad and the ugly. Cancer Metastasis Rev 2008; 27: 715-735.

29) Wiechen K, Sers C, Agoulnik A, Arlt K, Dietel M, Schlag PM, Schneider U. Down-regulation of caveolin-1, a candidate tumor suppressor gene, in sarcomas. Am J Pathol 2001; 158: 833-839.

30) Cantiani L, Manara MC, Zucchini C, De Sanctis P, Zuntini M, Valvassori L, Serra M, Olivero M, Di Renzo MF, Colombo MP. Caveolin-1 reduces osteosarcoma metastases by inhibiting c-Src activity and met signaling. Cancer Res 2007; 67: 7675-7685.

31) Jirawatnotai S, Hu Y, Livingston DM, Sicinski P. Proteomic identification of a direct role for cyclin d1 in DNA damage repair. Cancer Res 2012; 72: 4289-4293.

32) Alao JP. The regulation of cyclin D1 degradation: roles in cancer development and the potential for therapeutic invention. Mol Cancer 2007; 6: 24.

33) Xu H, Mei Q, Shi L, Lu J, Zhao J, Fu Q. Tumor-suppressing effects of miR451 in human osteosarcoma. Cell Biochem Biophys 2014; 69: 163-168.

34) Cai C-K, Zhao G-Y, Tian L-Y, Liu L, Yan K, Ma Y-L, Ji Z-W, Li X-X, Han K, Gao J. miR-15a and miR-16-1 downregulate CCND1 and induce apoptosis and cell cycle arrest in osteosarcoma. Oncol Rep 2012; 28: 1764-1770.

35) Shimada M. MicroRNA-mediated regulation of apoptosis in osteosarcoma. J Carcinogene Mutagene 2013; S6: 1-4.

36) Stehbens S, Wittmann T. Targeting and transport: how microtubules control focal adhesion dynamics. J Cell Biol 2012; 198: 481-489.

37) Alberti C. Apoptosis induction by quinazoline-derived alpha1-blockers in prostate cancer cells: biomolecular implications and clinical relevance. Eur Rev Med Pharmacol Sci 2007; 11: 59-64.

38) McLean GW, Carragher NO, Avizienyte E, Evans J, Brunton VG, Frame MC. The role of focal-adhesion kinase in cancer—a new therapeutic opportunity. Nat Rev Cancer 2005; 5: 505-515.

39) Golubovskaya VM. Focal adhesion kinase as a cancer therapy target. Anticancer Agents Med Chem 2010; 10: 735-741.

40) Schröder A, Delling G, Kaiser E. Expression analysis of protein tyrosine kinases of the FAK (focal adhesion kinase) family in osteosarcoma. Der Pathologe 2002; 23: 361-366.

41) Feng S, Shi X, Ren K, Wu S, Sun X. Focal adhesion kinase is involved in the migration of human osteosarcoma cells. Oncol Lett 2015; 9: 2670-2674.

42) Li J, Luo F, Zhang H, Li L, Xu Y. The CCND1 G870A polymorphism and susceptibility to bladder cancer. Tumor Biol 2014; 35: 171-177.

43) Liang W, Hao Z, Han J-L, Zhu D-J, Jin Z-F, Xie W-L. CAV-1 contributes to bladder cancer progression by inducing epithelial-to-mesenchymal transition. Urol Oncol 2014; 32: 855-863.

44) Aitken KJ, Bägli DJ. The bladder extracellular matrix. Part I: architecture, development and disease. Nat Rev Urol 2009; 6: 596-611.